Supplementary Information for

Active site profiling reveals coupling between domains in SRC-family kinases

Ratika Krishnamurty[1], Jennifer L. Brigham[1], Stephen E. Leonard[1], Pratistha Ranjitkar[1], Eric T. Larson[2], Edward J. Dale[1], Ethan A. Merritt[2], and Dustin J. Maly[1*]

Department of Chemistry[1]

University of Washington. Seattle, WA 98195. U.S.A.

Department of Biochemistry[2]

University of Washington. Seattle, WA 98195. U.S.A.

*Correspondence:

maly@chem.washington.edu (Tel: 206-543-1653/ FAX: 206-685-7002)

Supplementary Results

	IC_{50} (nM)
SRC	< 4
HCK	< 4
ABL	< 4

Supplementary Table 1. IC_{50} values for probe **1** in *in vitro* activity assays against protein kinases SRC, HCK, and ABL.

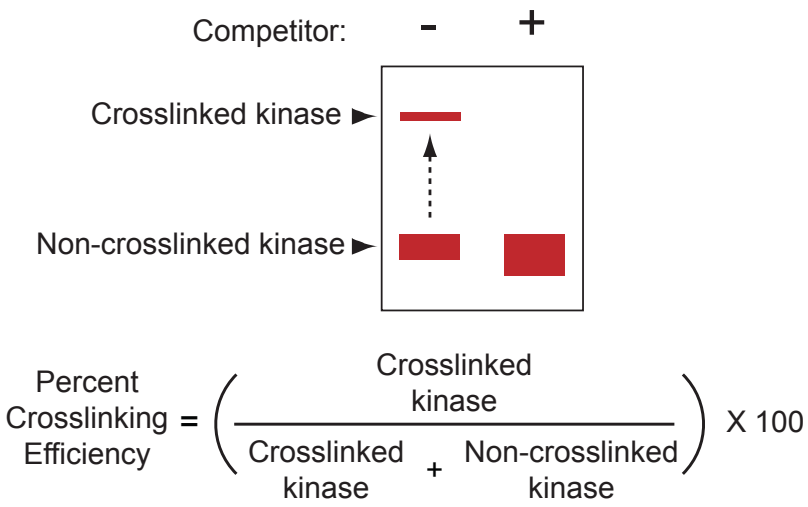

Supplementary Figure 1. Quantitation of kinase crosslinking efficiency. The increased size of the HaloTag-kinase complex allows the percentage of crosslinked kinase to be determined with a ratiometric gel-shift assay.

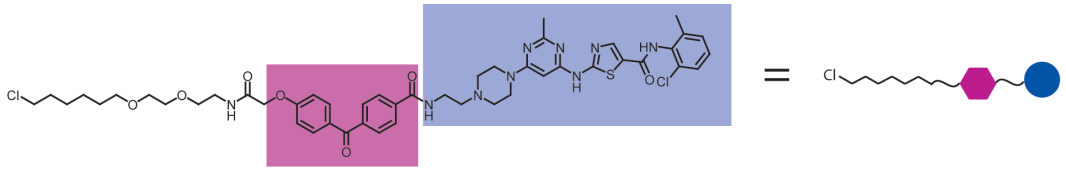

1

a. Post-conjugation Method:

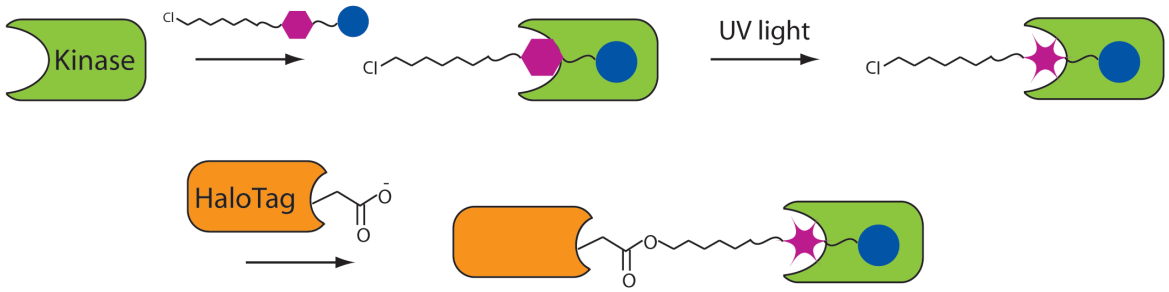

b. Pre-conjugation Method:

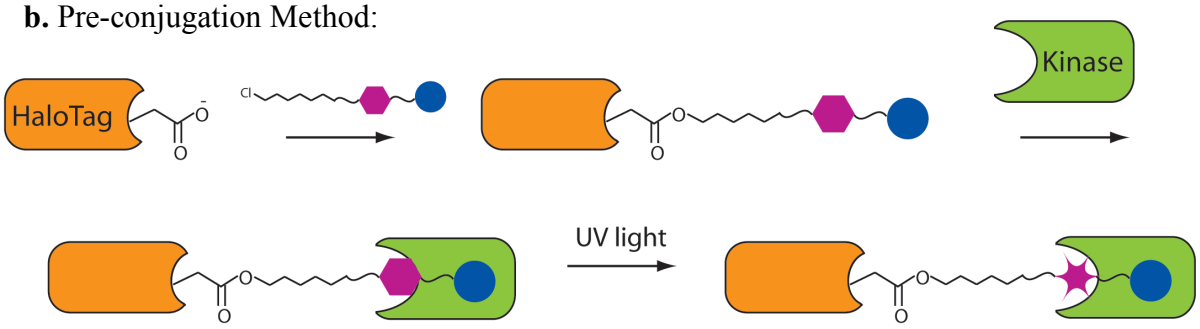

Supplementary Figure 2. Experimental crosslinking schematics using probe **1**. (a) In the post-conjugation method, probe **1** is first photo-crosslinked to the kinase. The probe **1**-kinase conjugate is then labeled with HaloTag. (b) In the pre-conjugation method, HaloTag is labeled with probe **1** prior to performing photo-crosslinking experiments. The HaloTag-probe **1** conjugate (HT-**1**) is then incubated with kinase and irradiated with UV light. Upon successful photo-crosslinking, a mass-shifted HaloTag-kinase complex is observed with both methods.

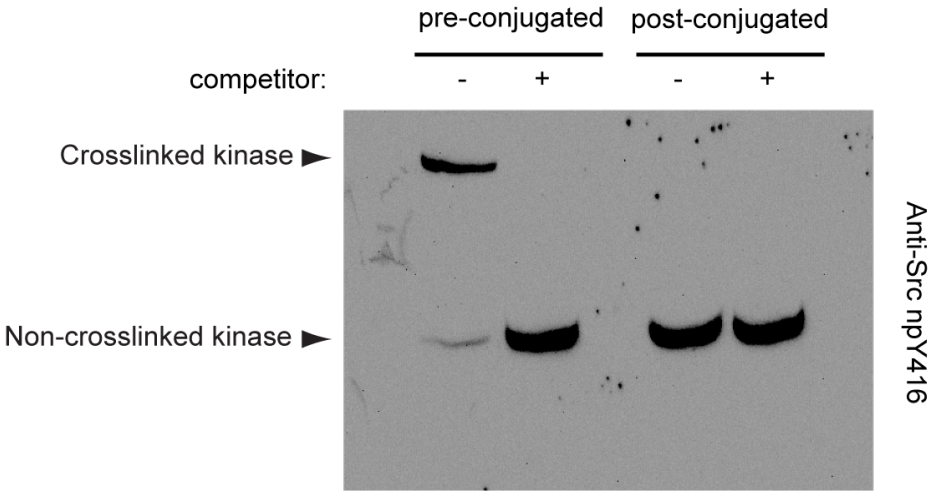

Supplementary Figure 3. Comparison of the pre- and post-conjugation photo-crosslinking methods as described in **Supplementary Figure 1**. Recombinant SRC (100 nM) was added to HeLa cell lysate (0.5 mg/ml) and subjected to the pre- and post-conjugation photo-crosslinking methods. After labeling, samples were subjected to SDS-PAGE separation, transferred to nitrocellulose, and then immunoblotted with an anti-SFK antibody (non-phospho-SFK (Tyr 416) (7G9), Cell Signaling). Significantly higher crosslinking efficiencies were consistently observed with the pre-conjugation method.

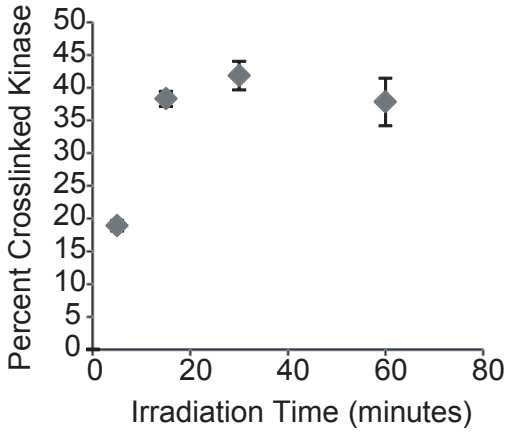

Supplementary Fig. 4. The effect of UV irradiation time on the crosslinking efficiency of HT-**1** with purified SRC (mean ± SEM, n = 3).

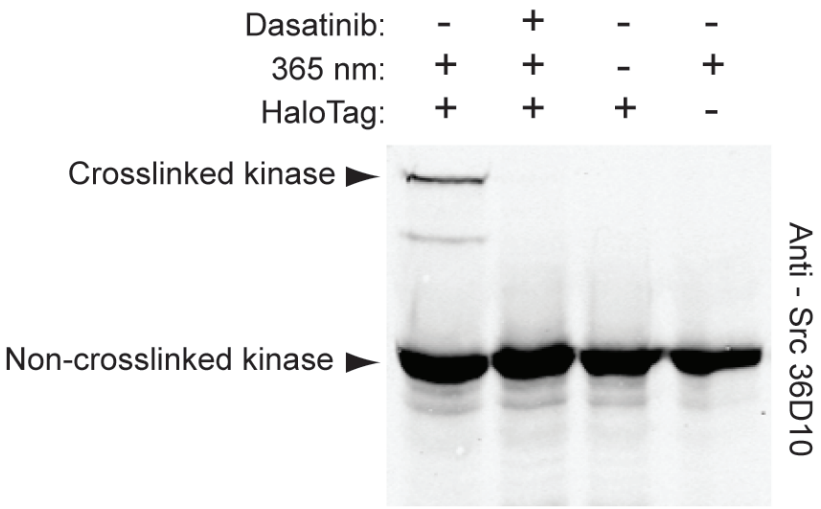

Supplementary Figure 5. Endogenous SFKs in live cells transiently expressing HaloTag are labeled by probe **1**. COS-7 cells transiently expressing HaloTag were incubated with probe **1** (1 μM) and then irradiated with UV light for eight minutes. Immunoblotting with an anti-SFK antibody (Src (36D10), Cell Signaling) shows the presence of mass-shifted SFKs (lane 1). Addition of an active site competitor prevents photo-crosslinking (lane 2). In the absence of UV irradiation, no mass-shifted SFKs are observed (lane 3), indicating that labeling is light dependent. Additionally, no mass-shifted kinases are observed when photo-crosslinking is performed in cells that are not transfected with HaloTag (lane 4).

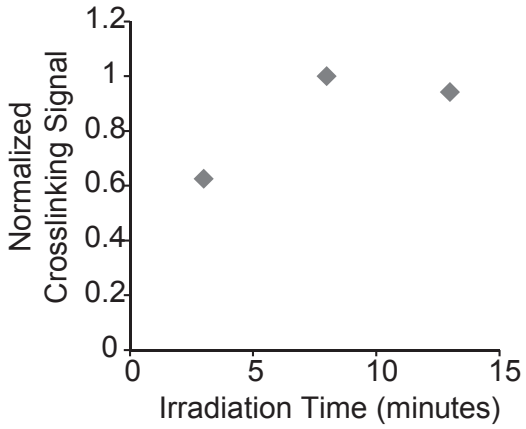

Supplementary Figure 6. The effect of UV irradiation time on SFK crosslinking in COS-7 cells. The experimental conditions described in **Supplementary Figure 5** were used. Normalized crosslinking signal is shown.

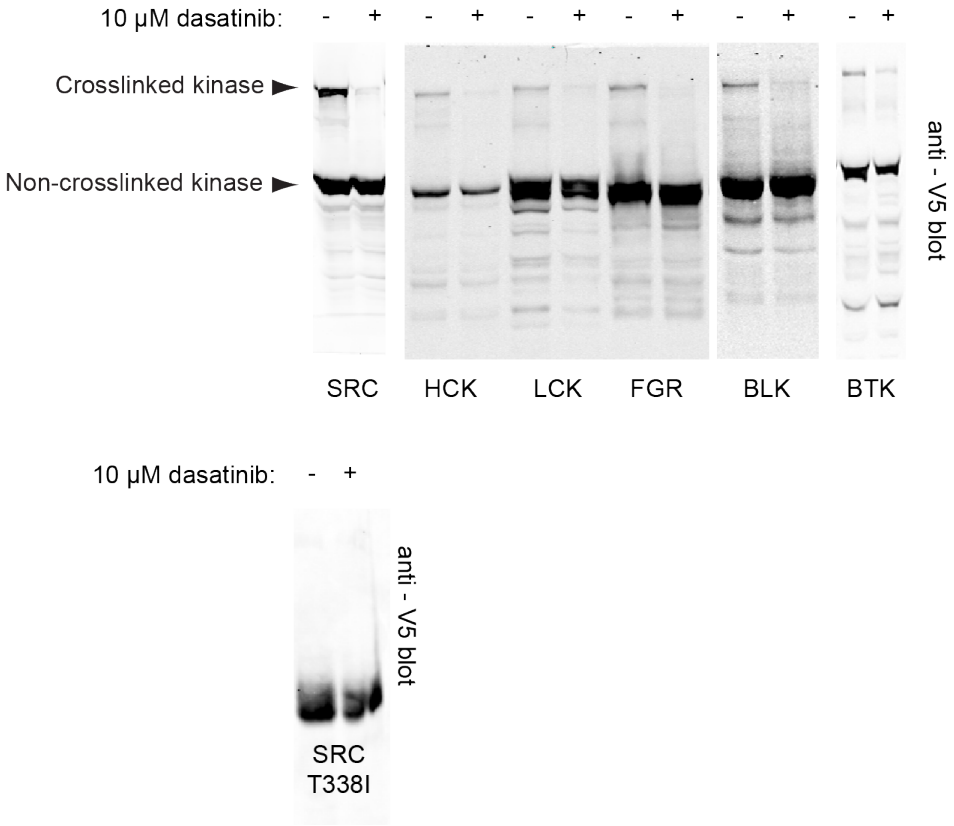

Supplementary Figure 7. Probe **1** labels non-receptor tyrosine kinases in COS-7 cells. COS-7 cells were co-transfected with a tyrosine kinase (pcDNA 3.2) and HaloTag (pDEST26). Cells were treated with 1 μM probe **1** for one hour and then irradiated with UV light for eight minutes. Western blot analysis with an anti-V5 antibody of the lysed cells following photo-crosslinking showed a mass-shifted HaloTag-kinase complex. In the presence of 10 μM dasatinib competitor, no mass-shifted kinases were observed. Furthermore, a mass-shifted band is absent when photo-crosslinking is performed with an ATP-binding site mutant of SRC (SRC^{T338I}) that does not bind dasatinib. These data show that photo-crosslinking in live cells is dependent upon binding to the kinase active site.

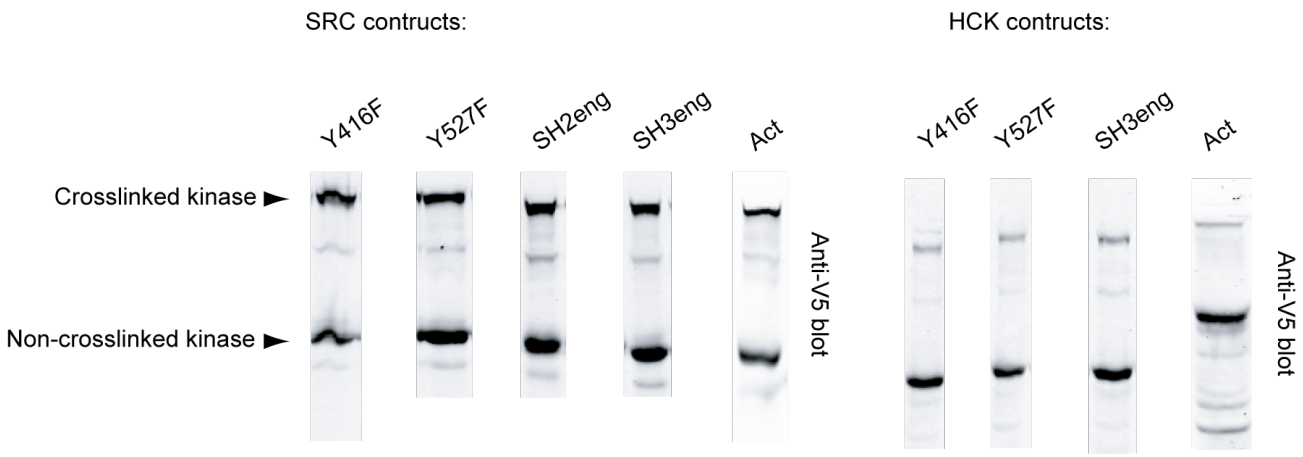

Supplementary Figure 8. Probe **1** labels SFK variants with diverse activation states in COS-7 cells. V5-tagged SRC and HCK constructs were co-expressed with HaloTag in COS-7 cells. Cells were incubated with probe **1** for one hour and then irradiated with UV light for eight minutes. Samples were immunoblotted using an anti-V5 antibody and the percent crosslinked kinase was determined. All of the SRC variants were labeled with similar crosslinking efficiencies (35-45%). All of the HCK variants were labeled with similar crosslinking efficiencies (11-17%).

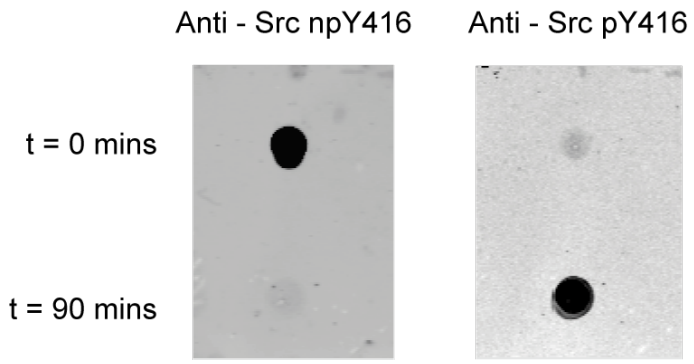

Supplementary Figure 9. Activation loop auto-phosphorylation of purified SRC^{Y527F}. Purified SRC^{Y527F} was incubated with 1 mM ATP at 37 °C for 90 minutes. Immunoblotting with a phospho-specific antibody (phospho-SFK (Tyr416), Cell Signaling) demonstrated efficient activation loop phosphorylation. The absence of a signal using an antibody that is specific for the non-phosphorylated activation loop of SFKs (non-phospho-SFK (Tyr 416) (7G9), Cell Signaling) shows that activation loop phosphorylation is quantitative under these conditions. The same conditions were used to activate HCK^{Y527F}.

	K_i (nM)			
	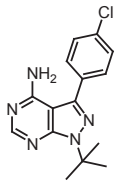	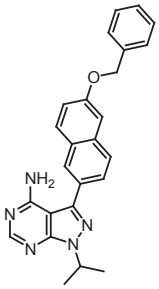	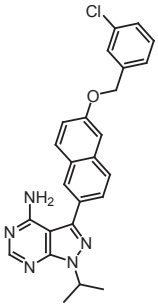	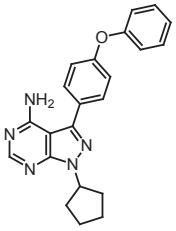
	7 (PP2)	**8**	**9**	**10**
SRC^{Act}	43 ± 3	1200 ± 100	1400 ± 100	110 ± 10
SRC^{SH2eng}	87 ± 12	190 ± 50	44 ±1	< 20
HCK^{Act}	31 ± 3	1100 ± 200	3200 ± 300	83 ± 10
HCK^{SH2eng}	67 ± 11	58 ± 6	16 ± 2	< 15
HCK^{SH3eng}	53 ± 3	30 ± 3	< 15	< 15

Supplementary Figure 10. K_i values (nM) of inhibitors **7-10** for SRC^{Act}, SRC^{SH2eng}, HCK^{Act}, HCK^{SH2eng}, and HCK^{SH3eng}. Inhibitors **7-10** were tested in an *in vitro* activity assay for their abilities to inhibit SRC^{Act}, SRC^{SH2eng}, HCK^{Act}, HCK^{SH2eng}, and HCK^{SH3eng}. IC_{50} values were converted to K_i values using the Cheng−Prusoff equation[1].

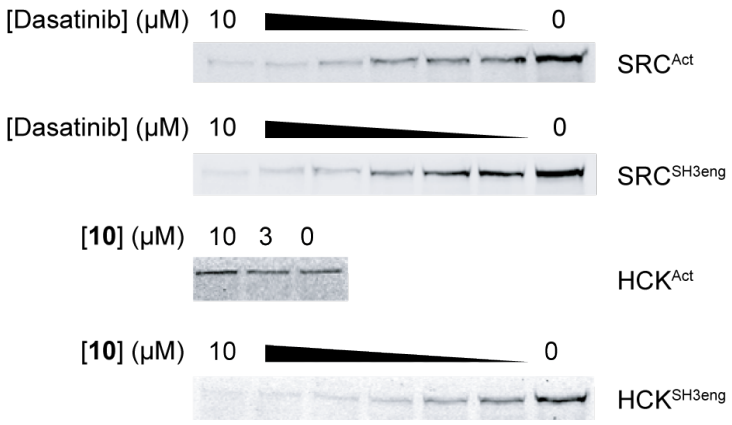

Supplementary Figure 11. Representative Western blots for cellular competition experiments with probe **1** against SFK variants transiently expressed in COS-7 cells. The amount of mass-shifted kinase at each inhibitor concentration is measured to obtain a cellular IC_{50} value for photo-crosslinking competition. Cellular competition experiments with SRC variants (SRC^{Act} and SRC^{SH3eng}) and increasing concentrations of dasatinib are shown in the top panels. Cellular competition experiments with HCK variants (HCK^{Act} and HCK^{SH3eng}) and increasing concentrations of inhibitor **10** are shown in the bottom panels.

IC_{50} (nM)	Dasatinib	**10**
SRC^{Act}	20 ± 9	>3000
SRC^{SH3eng}	45 ± 2	620 ± 20
HCK^{Act}	36 ± 12	>3000
HCK^{SH3eng}	420 ± 60	44 ± 3

Supplementary Figure 12. The IC_{50} values (mean ± SEM, n = 3) used to calculate the fold differences shown in **Figure 4b**.

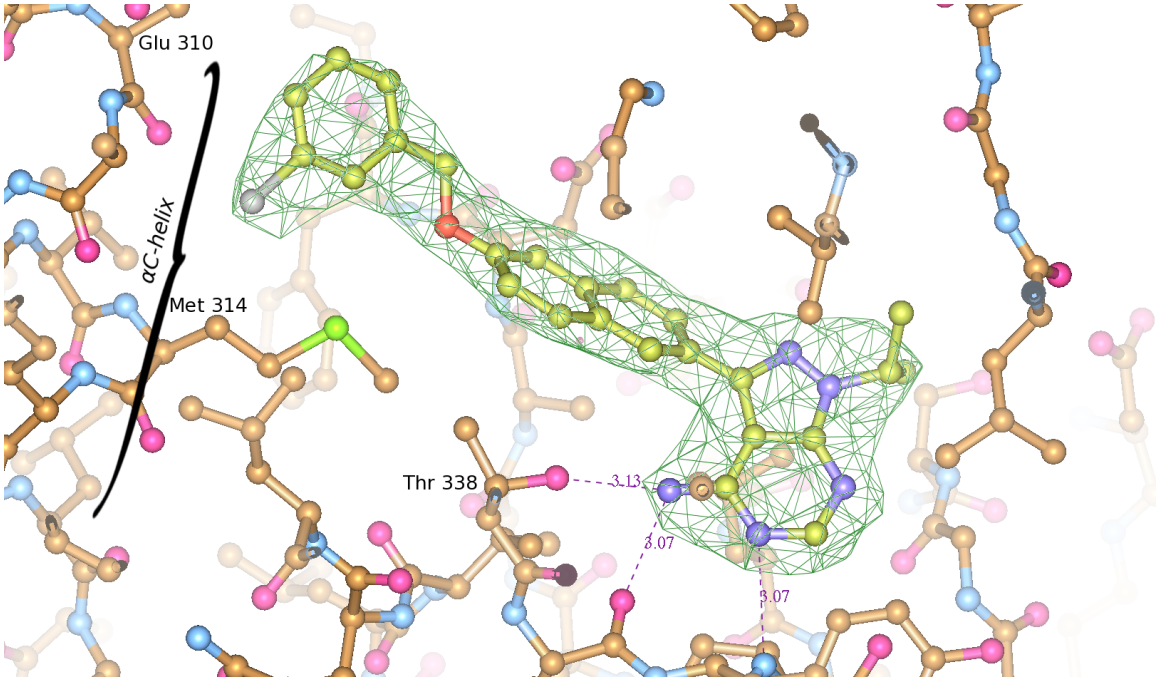

Supplementary Figure 13. Difference electron density (mFo-Fc) calculated from the final crystallographic model with inhibitor atoms omitted during calculation of Fc. The contour level corresponds to 3σ in the overall difference map, but only the density in the region of the inhibitor is shown.

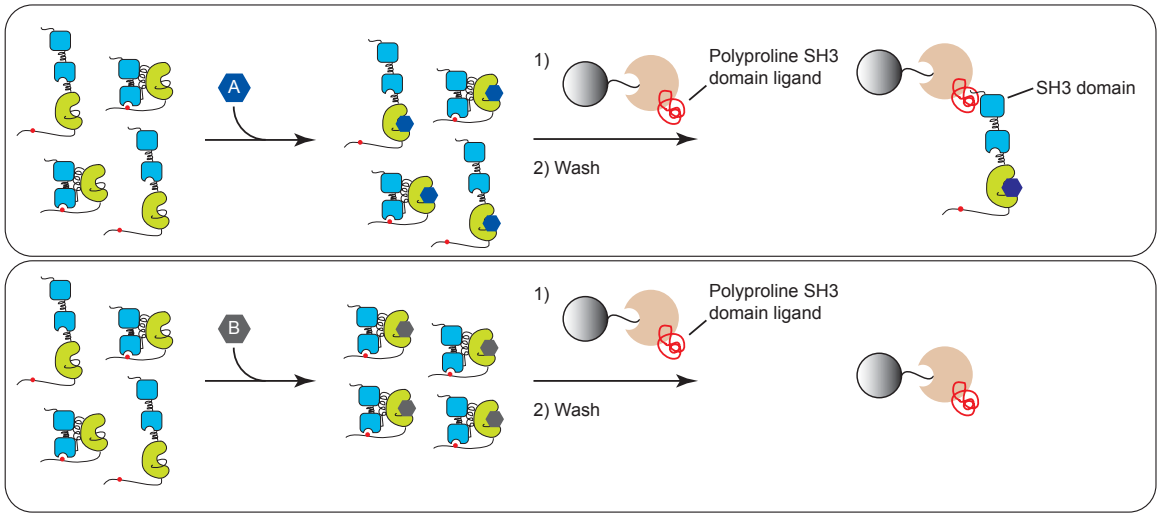

Supplementary Figure 14. Pull-down assay to determine the SH3 domain accessibilities of SRC and HCK. Beads containing a polyproline (PP) SH3 domain ligand are incubated with inhibitor-bound kinases. The beads are then washed and the amount of bound SFK is determined following elution. Two possible results are shown. In the top panel, an ATP-competitive inhibitor, **A**, does not affect the SH3 domain accessibility of the SFK tested. This results in the SH3 domains of some inhibitor-bound SFKs being able to engage in an inter-molecular interaction and retention of these kinases on PP ligand-containing beads. In the bottom panel, an ATP-competitive inhibitor, **B**, influences the SH3 domain of an inhibitor-bound SFK to engage intra-molecularly. As a result, no inhibitor-bound kinases are retained on the beads.

	Percent kinase eluted	
	SRC	HCK
Dasatinib	22 ± 2	27 ± 2
2	75 ± 5	5.7 ± 1.9
8	4.3 ± 0.4	0
9	0	1.0 ± 0.5
10	2.4 ± 0.5	0

Supplementary Figure 15. Values used for the graphical representation of the pull-down data shown in **Figure 6b**.

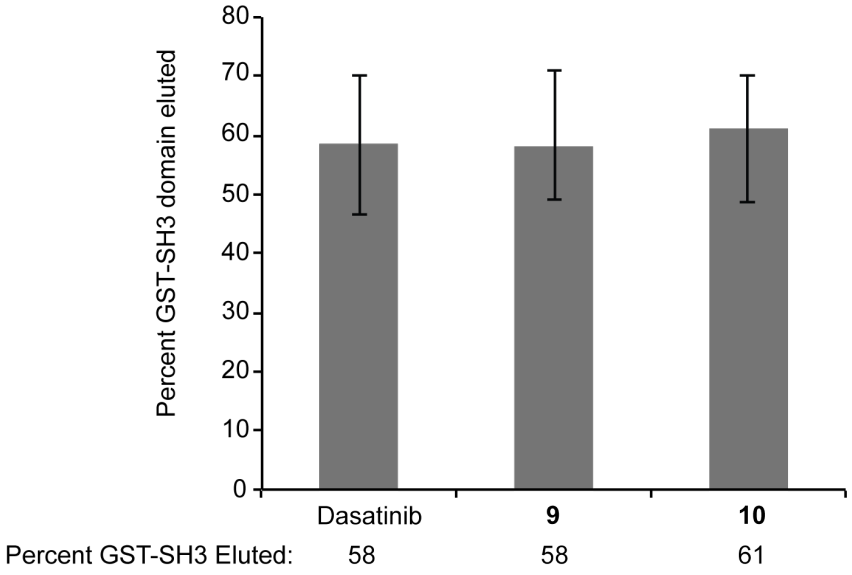

Supplementary Figure 16. Pull-down experiments with the SH3 domain of HCK (GST-SH3(HCK)). To ensure that the observed SH3 domain inaccessibility of SRC and HCK in the presence of **8-10** is due to the interaction of these inhibitors with the ATP-binding sites of these kinases, pull-down experiments with the isolated SH3 domain of HCK (GST-SH3) were performed. GST-SH3 domain was incubated with either dasatinib, **9**, or **10** and subjected to the pull-down protocol described in the **Methods** section. Dasatinib, **9**, and **10** were used at the same concentrations as the experiments performed in **Figure 6**. The percent of SH3 domain that was retained on the resin was determined via immunoblotting eluted samples with an anti-GST antibody (mean ± SEM, n = 3).

	K_d (μM)	
	+ dasatinib (30 μM)	+ **10** (60 μM)
SRC	2.2 ± 0.4	> 25
HCK	3.0 ± 0.3	> 25

Supplementary Figure 17. The binding affinities of inhibitor-bound SRC^{Y527F} and HCK^{Y527F} for an SH3 peptide ligand. K_d values (μM) were determined by monitoring the change in fluorescence polarization of a fluorescently-labeled SH3 peptide ligand (FAM-AAVSLARRPLPPLP-NH_2) in the presence of increasing concentrations of SRC^{Y527F} and HCK^{Y527F}. Assays were run in the presence of a saturating concentration of dasatinib (30 μM) or inhibitor **10** (60 μM). Values shown are the average of three assays ± SEM.

a

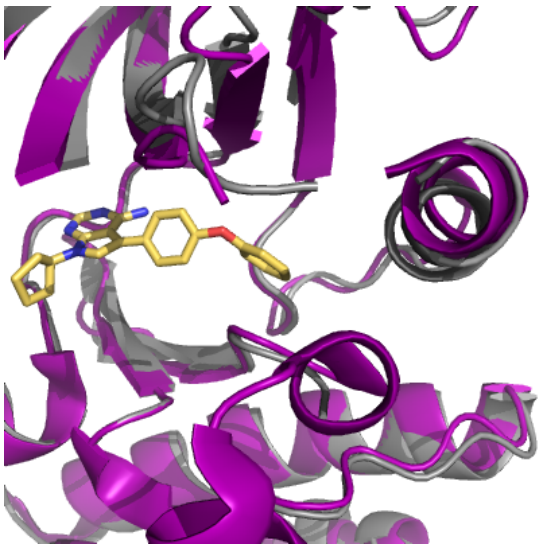

b

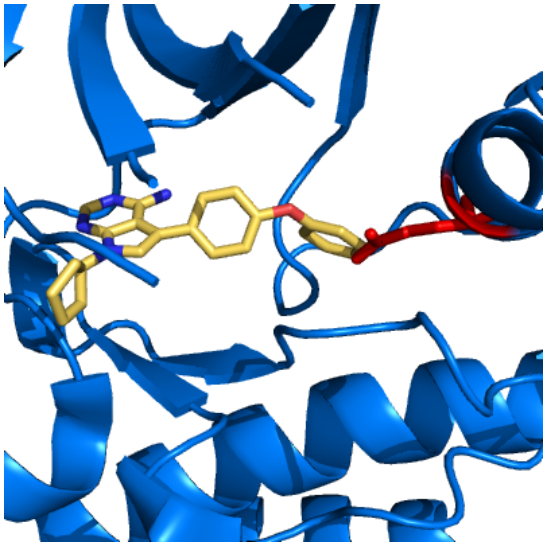

Supplementary Figure 18. SRC and BTK adopt the SRC/CDK-like inactive conformation when bound to inhibitors **9** and **10**, respectively. (a) Superposition of BTK (grey) in complex with **10** (yellow) (PDB code 3GEN) and SRC (purple) in complex with **9** (inhibitor **9** is not shown). The conformations of the ATP-binding sites of the two kinases align with one another, as both adopt the SRC/CDK-like inactive conformation. Notably, the helix αCs of both kinases undergo the same conformational change by swinging out of the ATP-binding site. This allows the diphenyl ether of inhibitor **10** to occupy the hydrophobic pocket created by helix αC movement. (b) Superposition of inhibitor **10** (yellow) bound to BTK and the active form of SRC (SRC-dasatinib (PDB code 3G5D) (blue)). BTK must adopt the SRC/CDK-like inactive conformation to accommodate **10**. SRC would be predicted to adopt a similar conformation to prevent a steric clash between the helix αC and the diphenyl ether.

Supplementary Table 2. Data collection and refinement statistics.

	PDB 4DGG
Data collection	
Space group	P1
Cell dimensions	
a, *b*, *c* (Å)	42.17, 63.48, 74.00
α, β, γ (°)	78.73, 88.48, 89.93
Resolution (Å)	2.65 (2.79-2.65) *
R_{pim}	0.116 (0.604)
$I / \sigma I$	6.2 (1.7)
Completeness (%)	81 (73)
Redundancy	3.8 (3.7)
Refinement	
Resolution (Å)	2.65
No. reflections	16811/866
R_{work} / R_{free}	0.208/0.252
No. atoms	
Protein	4179
Ligand/ion	64
Water	13
B-factors	
Protein (B_{eq})	39
Ligand/ion (B_{iso})	46
Water (B_{iso})	21
R.m.s. deviations	
Bond lengths (Å)	0.009
Bond angles (°)	1.304

*Highest-resolution shell is shown in parentheses.

[AU: Equations defining various R values are standard and hence are no longer defined in the footnotes.]
[AU: Ramachandran statistics should be in methods section at the end of the refinement sub-section.]
[AU: Wavelength of data collection, temperature, beamline should all be in methods section.]

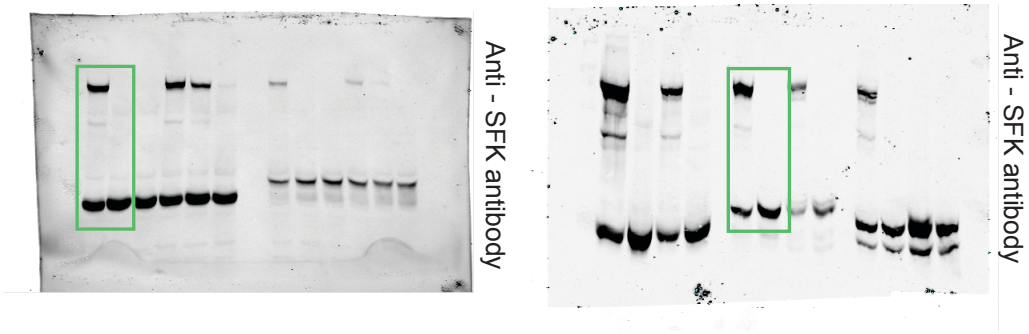

Supplementary Figure 19. Full uncropped blots for **Figure 1d**.

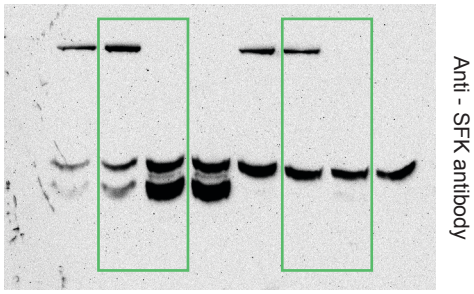

Supplementary Figure 20. Full uncropped blots for **Figure 2a**.

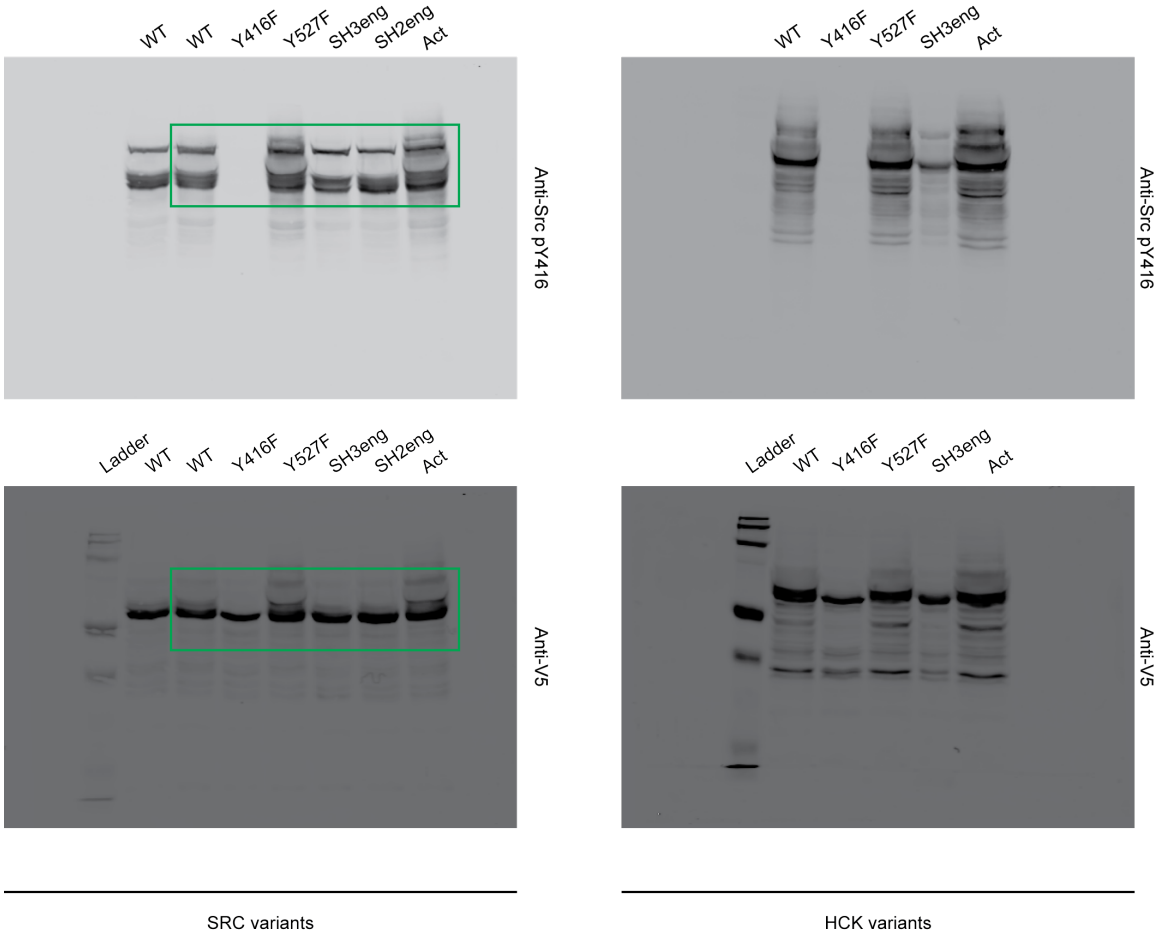

Supplementary Figure 21. Full uncropped blots for **Figure 3b**.

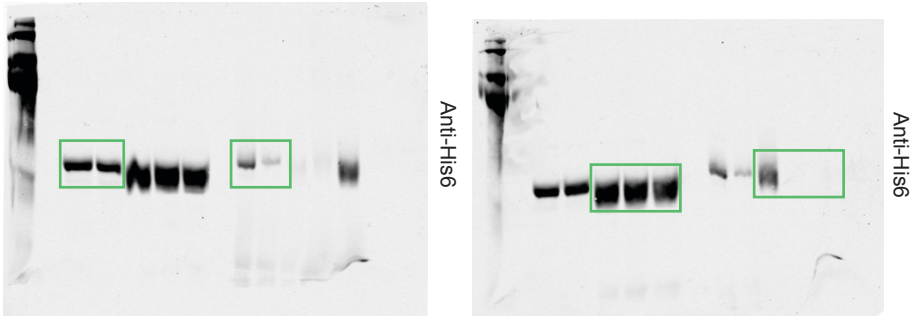

Supplementary Figure 22. Full uncropped blots for **Figure 6a**.

Supplementary Methods

General: Commercially available reagents and anhydrous solvents were used without further purification unless otherwise specified. The purities of all finals compounds were determined by analytical HPLC with an Agilent ZORBAX SB-C_{18} column (2.1 mm x 150 mm) in two different solvent systems (MeOH/water and acetonitrile/water). *Analytical HPLC Conditions:* C_{18} column (150 x 2.1 mm), Acetonitrile/Water-0.05% CF_3CO_2H gradient: 2:98 to 100:0 over 30 min. MeOH/Water–0.05% CF_3CO_2H gradient: 2:98 to 100:0 over 30 min. Flow rate = 1 mL/min; 220 and 254 nM detection for 30 min. All compounds were determined to be >95% pure in both solvent systems. Flash chromatography was performed on prepacked columns of silica gel (Varian SF10-4g, Si 50) by IntelliFlash with EtOAc/hexanes, MeOH/$CHCl_3$ or MeOH/CH_2Cl_2 as eluent. Purifications by preparative HPLC were performed on a Varian Dynamax Microsorb 100-5 C_{18} column (250 mm x 21.4 mm). Acetonitrile/Water–0.05% CF_3CO_2H gradient: 1:99 to 100:0 over 60 min; 8 mL/min; 254 nm detection for 60 min or MeOH/Water–0.05% CF_3CO_2H gradient: 1:99 to 100:0 over 60 min; 8 mL/min; 254 nm detection for 60 min. Mass spectra were recorded with the Bruker Esquire Liquid Chromatograph - Ion Trap Mass Spectrometer. NMR spectra were recorded with either a Bruker AV300 or Bruker AV500 instrument at ambient temperature with the residual solvent peaks as internal standards. Chemical shifts are reported in ppm (δ) and coupling constants are reported in Hz. ^1H resonances are referenced to $CDCl_3$ (7.26 ppm), DMSO-d_6 (2.54) or CD_3OD (3.34).

Synthetic Experimental Procedures and Characterization:

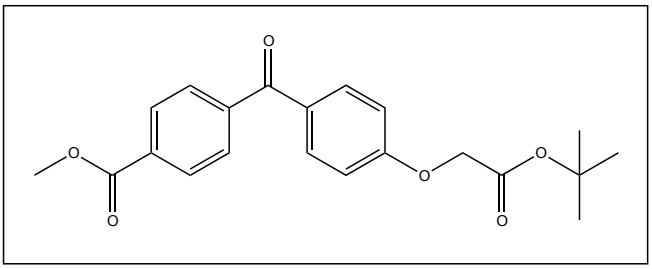

methyl 4-(4-(2-tert-butoxy-2-oxoethoxy)benzoyl)benzoate (11)

(11) Under a nitrogen atmosphere, methyl 4-(4-hydroxybenzoyl)benzoate[2] (284 mg, 1.11 mmol, 1 equiv.), *tert*-butyl bromoacetate (216 mg, 1.11 mmol, 1 equiv.), potassium carbonate (306 mg, 2.22 mmol, 2 equiv.), tetrabutylammonium iodide (36.9 mg, 0.100 mmol, 0.09 eqiv.), and acetonitrile (2.3 ml) were combined. The resulting mixture was heated to 70 °C. After 3 hours, the reaction was cooled in an ice-water bath. The reaction was then concentrated under reduced pressure. The concentrate was dissolved in dichloromethane, washed with water (2x) and dried over Na_2SO_4. The solvent was evaporated under reduced pressure to yield **methyl 4-(4-(2-tert-butoxy-2-oxoethoxy)benzoyl)benzoate (11)** as a pale yellow solid (373 mg, 91% yield). TLC (EtOAc:hexanes, 30:70 v/v): $R_f = 0.5$; ^{1}H NMR (300 MHz, $CDCl_3$) δ 1.43 (s, 9H), 3.90 (s, 3H), 4.54 (s, 2H), 6.90 (d, $J = 9.0$ Hz, 2H), 7.71-7.76 (m 4H), 8.08 (d, $J = 9.0$ Hz, 2H). ^{13}C NMR (125 MHz, $CDCl_3$) δ 28.4, 52.8, 65.9, 83.2, 114.7, 129.8, 129.8, 130.7, 132.9, 133.2, 142.3, 162.2, 166.7, 167.6, 195.0. ESI (MS) Calculated for $C_{21}H_{23}O_6$ [M+H$^+$]: 371.1, found: 371.3.

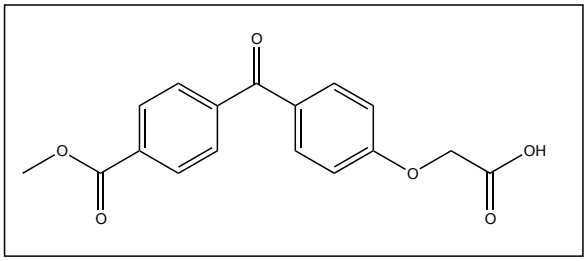

2-(4-(4-(carbonyl)benzoyl)phenoxy)acetic acid (12)

(12) 11 (373 mg, 1.01 mmol) was dissolved in a mixture of dichloromethane (1.9 ml) and trifluoroacetic acid (970 µl) at 0 °C. The reaction was allowed to warm to room temperature and stirred for three hours. Toluene (1.0 ml) was then added to the reaction and the solvent was evaporated under reduced pressure to yield **2-(4-(4-(carbonyl)benzoyl)phenoxy)acetic acid (12)** (317 mg, 100% yield). The product was used in the next step without further purification. TLC (AcOH:CH_3OH: CCl_3H, 1:10:89 v/v): $R_f = 0.5$; ^{1}H NMR (300 MHz, $CDCl_3$) δ 3.99 (s, 3H), 4.81 (s, 2H), 7.04 (d, $J = 9.1$ Hz, 2H), 7.81-7.88 (m, 4H), 8.17 (d, $J = 7.9$ Hz, 2H). ^{13}C NMR (125 MHz, D6-DMSO) δ

52.5, 64.7, 114.6, 129.2, 129.4, 132.2, 132.2, 141.7, 161.9, 165.7, 169.7. 193.8. ESI (MS) Calculated for $C_{17}H_{15}O_6$ [M+H$^+$]: 315.1, found: 315.4.

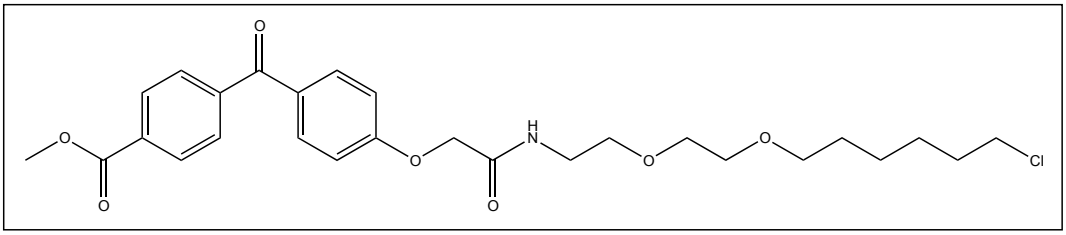

methyl 4-(4-(2-(2-(2-(6-chlorohexyloxy)ethoxy)ethylamino)-2-oxoethoxy)benzoyl)benzoate (13)

(13) 12 (40 mg, 0.13 mmol, 1 equiv.) and 2-[2-[(6-chlorohexyl)oxy]ethoxy]ethanamine[3] (37 mg, 0.17 mmol, 1.3 equiv.) were dissolved in DMF (243 µl) at 0 °C. HOAt (22 mg, 0.17 mmol, 1.3 equiv.), DIEA (67 µl, 0.38 mmol, 3 equiv.) and EDCI (32 mg, 0.17 mmol, 1.3 equiv.) were added sequentially and the reaction was stirred at room temperature overnight. The reaction was then diluted in EtOAc, washed with K_2CO_3 and saturated NH_4Cl. Purification of the crude product on silica (EtOAc/hexanes) afforded **13** (34 mg, 52% yield). TLC (EtOAc:hexanes, 60:40 v/v): R_f = 0.15; ^{1}H NMR (300 MHz, $CDCl_3$) δ 1.31-1.36 (m, 4H), 1.52 (m, 2H), 1.68 (m, 2H), 3.48-3.61 (m, 12H), 3.90 (s, 3H), 4.52 (s, 2H), 6.95 (d, 2H, *J* = 9.0 Hz), 7.74 (d, 2H, *J* = 9.0 Hz), ^{13}C NMR (125 MHz, $CDCl_3$) δ 25.8, 27.0, 29.8, 32.9, 39.3, 45.4, 52.9, 67.6, 70.0, 70.4, 70.8, 71.7, 114.9, 129.9, 129.9, 131.3, 133.1, 133.4, 142.0, 161.2, 166.7, 168.0, 195.0. ESI (MS) Calculated for $C_{27}H_{34}ClNO_7$ [M+H$^+$]: 520.2, found [M+K$^+$]: 558.5.

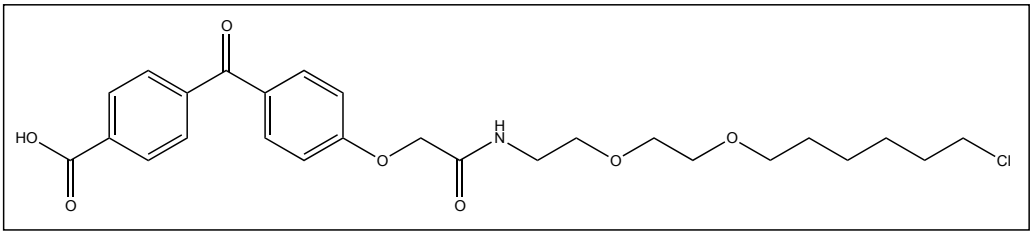

4-(4-(2-(2-(2-(6-chlorohexyloxy)ethoxy)ethylamino)-2-oxoethoxy)benzoyl)benzoic acid (14)

(14) LiOH (6.0 mg, 0.14 mmol, 3.0 equiv.) was added to **12** (23.8 mg, 0.046 mmol, 1.0 equiv.) in a 1:1 mixture of THF and water (1 ml). The mixture was stirred at room temperature and reaction progress was monitored with TLC. Upon completion, the solvent was removed *in vacuo*. The resultant residue was taken up in water and the aqueous phase acidified with 1M HCl until a white precipitate formed. The acid was extracted into EtOAc and the organic phase concentrated to provide **14** as a white solid (20.2 mg, 87%). Due to its instability, **14** was immediately carried onto the next step. TLC (1% Acetic acid in EtOAc:hexanes, 80:20 v/v): R_f = 0.10; ^{1}H NMR (300 MHz, CD_3OD) δ 1.33-1.42 (m, 4H), 1.58 (m, 2H), 1.74-1.80 (m, 2H), 3.45-3.51 (m, 6H), 3.58-3.61 (m, 6H), 4.67 (s, 2H), 7.15 (d, 2H, *J* = 9.0 Hz), 7.82 (d, 2H, *J* = 8.4 Hz), 7.86 (d, 2H,

J = 9.0 Hz), 8.18 (d, 2H, J = 8.4 Hz). ESI (MS) Calculated for $C_{26}H_{33}ClNO_7$ [M+H$^+$]: 506.2, found: 506.2.

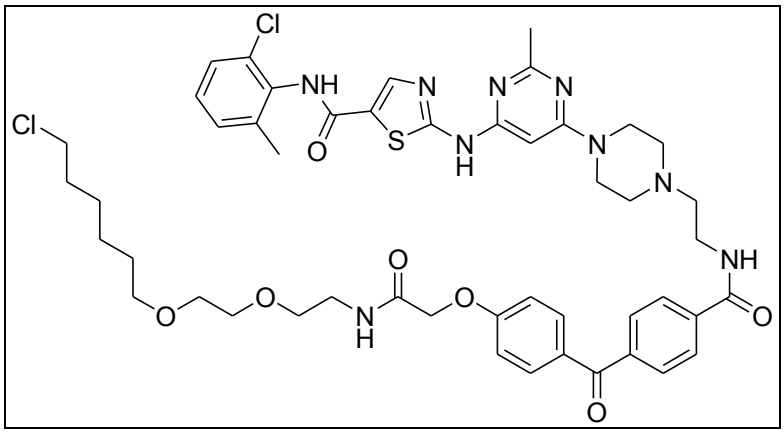

N-(2-chloro-6-methylphenyl)-2-(6-(4-(2-(4-(4-(2-(2-(2-(6-chlorohexyloxy) ethoxy)ethylamino)-2-oxoethoxy)benzoyl)benzamido)ethyl)piperazin-1-yl)-2-methylpyrimidin-4-ylamino)thiazole-5-carboxamide (probe 1)

(1) 2-[6-[4-(2-aminoethyl)-1-piperazinyl]]-2-methyl-4-pyrimidinyl]amino]-N-(2-chloro-6-methylphenyl)-5-thiazolecarboxamide[3] (7.9 mg, 0.013 mmol, 1.0 equiv.) and **14** (8.7 mg, 0.017 mmol, 1.3 equiv.) were dissolved in DMF. HOBt (2.6 mg, 0.017 mmol, 1.3 equiv.), DIEA (5 μl, 0.034 mmol, 2.0 equiv.) and EDCI (2.7 mg, 0.017 mmol, 1.3 equiv.) were added sequentially and the reaction was stirred at room temperature overnight. The crude reaction mixture was dissolved in 5 mL of 1:1 acetonitrile/water and purified by preparative HPLC to afford probe **1** (4.42 mg, 32%). **1** was found to be >95% pure by analytical HPLC (traces shown below). ^{1}H NMR (500 MHz, CD_3OD) δ 1.33-1.41 (m, 6H), 1.58 (m, 2H), 1.74 (m, 2H), 2.35 (s, 3H), 2.53 (s, 3H), 3.43 (m, 3H), 3.50-3.59 (m, 6H), 3.62-3.68 (m, 5H), 3.70-3.76 (m, 5H), 3.78 (m, 3H), 4.75 (s, 2H), 6.16 (s, 1H), 7.20 (d, 2H, J = 10.0 Hz), 7.28 (m, 2H), δ 7.39 (m, 1H), 7.82 (d, 2H, J = 5.0 Hz), 7.88 (d, 2H, J = 10.0 Hz), 7.99 (d, 2H, J = 10.0 Hz), 8.20 (s, 1H). ^{13}C NMR (125 MHz, CD_3OD) δ 18.8, 25.6, 26.5, 27.8, 30.6, 33.8, 35.2, 41.2, 42.5, 45.8, 49.2, 49.5, 68.3, 70.5, 71.3, 71.4, 72.3, 84.7, 87.9, 103.1, 115.8, 122.7, 126.8, 128.5, 129.6, 130.2, 130.8, 131.9, 132.1, 133.8, 139.0, 140.4, 141.9, 148.8, 156.3, 158.9, 160.0, 163.0, 163.8, 165.1, 167.8, 169.4, 172.1, 178.0, 183.8, 184.9, 188.6, 196.5. ESI (MS) Calculated for $C_{48}H_{57}Cl_2N_9O_7S$ [M+H$^+$]: 975.0, found: 974.9.

Probe **1:** Analytical HPLC trace: Acetonitrile/Water

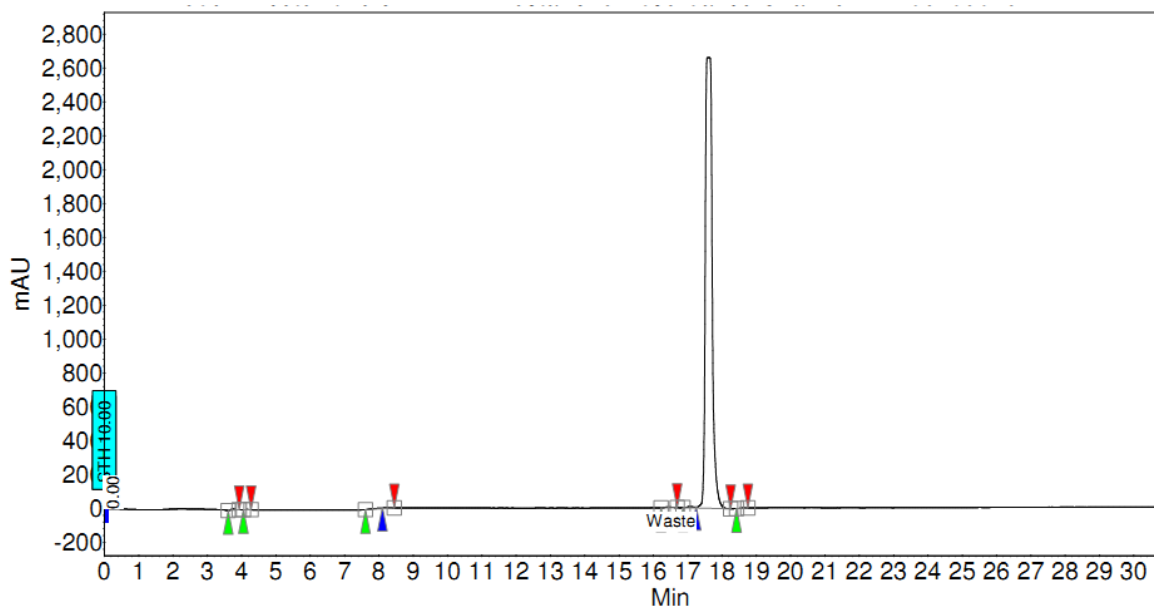

Probe **1:** Analytical HPLC trace: MeOH/Water

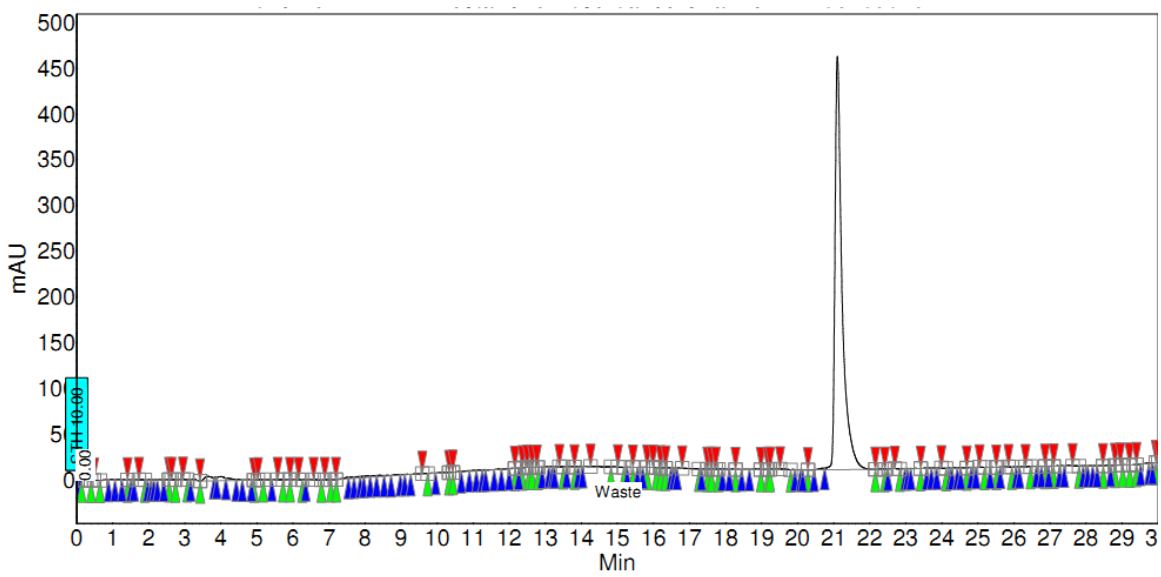

^{1}H NMR) of probe **1.**

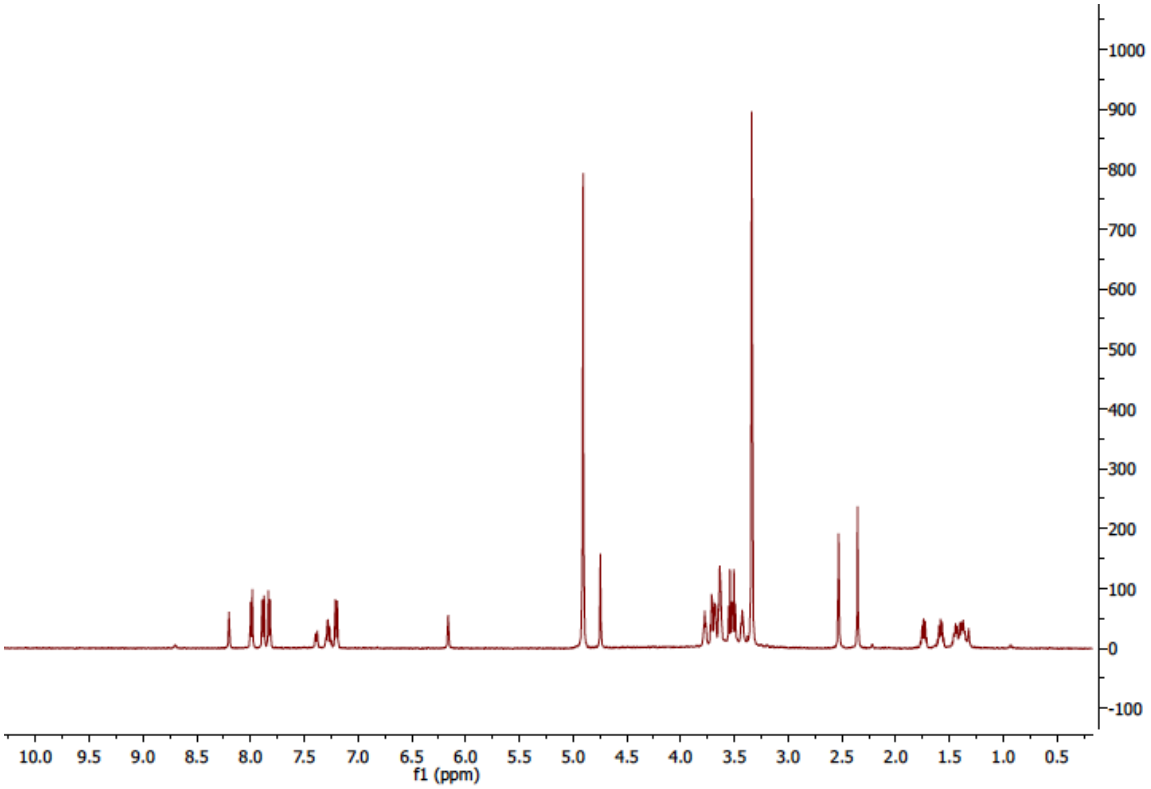

ATP-competitive inhibitors 2-10

Inhibitors **2**, **4**, **5**, and dasatinib were obtained from a commercial supplier (ChemieTek). Inhibitor **3** was made according to a previously published procedure[4]. Inhibitors **6-10** were made according to a previously published procedure[5]. All spectral data matches previously reported inhibitor characterization. All inhibitors were verified to be >95% pure by analytical HPLC.

SFK construct expression and purification

Coomassie-stained gels of purified SFK constructs are shown below:

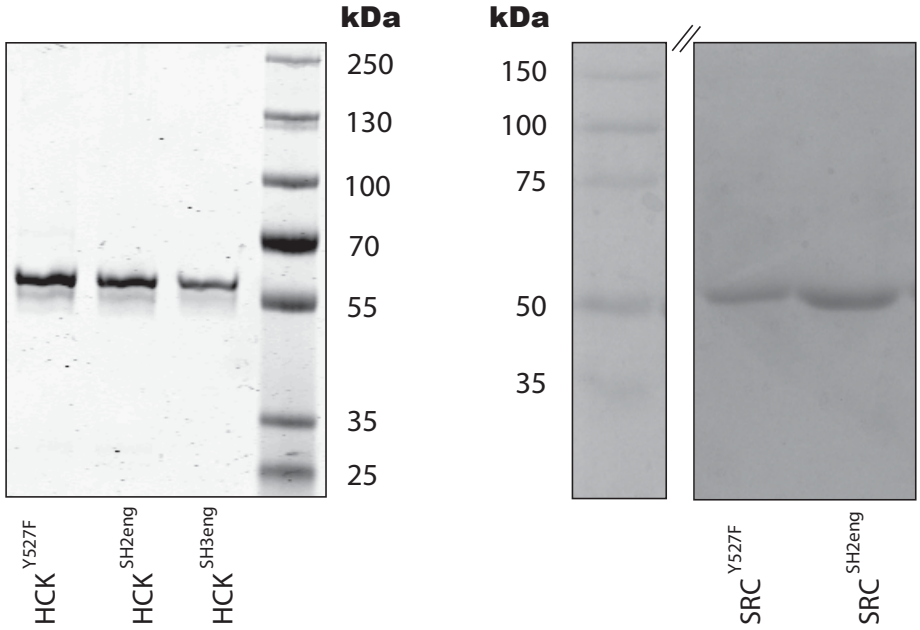

***In vitro* activity assays**

Inhibitors were assayed in triplicate against each kinase ([SRC] = 4 nM, [HCK] = 4 nM, [ABL] = 4 nM, [SRC^{Act}] = 1 nM, [HCK^{Act}] = 1 nM, [SRC^{SH2eng}] = 20 nM, [HCK^{SH2eng}] = 15 nM, [HCK^{SH3eng}] = 15 nM) in assay buffer containing 75 mM HEPES, pH = 7.5, 15 mM $MgCl_2$, 3.75 mM EGTA, 150 mM NaCl, 0.2 mg/mL BSA, γ32P-ATP (0.2 μCi/well) and an optimized SRC peptide substrate (Ac-EIYGEFKKK-OH, final concentration = 130 μM) or ABL peptide substrate (Ac-EAIYAAPFAKKK, final concentration = 130 μM). The enzymatic reaction was run at room temperature for two hours and then terminated by spotting onto a phosphocellulose membrane. Membranes were washed, dried, and the radioactivity was determined by phosphorimaging with a Storm 840 phosphor scanner. The scanned membranes were quantified with ImageQuant and converted to percent inhibition. Data were analyzed using Prism Graphpad software and IC_{50} values were determined using non-linear regression analysis.

Preparation of a fluorophore-labeled HaloTag fusion construct for *in vitro* competition experiments

A fusion construct was made that linked the SNAP-tag AGT gene (NEB) to the HaloTag gene (pFC8K vector, Promega) via a SUMO linker. The SUMO gene was amplified from a plasmid containing the SMT3/SUMO gene (Plasmid 16092: pT-35 Addgene) with primers that included a 5' end complementary to the 3' end of AGT and a 3' end complementary to the 5' end of HaloTag. The complete construct was then incorporated into the vector pMCSG7 (Midwest Center for Structural Genomics) by ligation independent cloning. This HaloTag fusion construct was expressed in *E. coli* and purified. This fusion construct allowed for conjugation to probe **1** via HaloTag and subsequent conjugation to a benzylguanine-linked fluorescein substrate via SNAP-tag after photo-crosslinking experiments were performed.

HaloTag Fusion Construct Expression

Single colonies of BL21(DE3) cells transformed with the plasmid were grown overnight in 6 mL LB supplemented with ampicillin (100 µg/mL) at 37 °C. Overnight cultures were then centrifuged at 3000 x g for 6 minutes at 4 °C. The media was decanted and the cell pellet was re-suspended in 2 mL of LB and transferred to 1 L LB (with 100 µg/mL ampicillin). The bacterial culture was grown at 37 °C to an OD_{600nm} of 0.8-1.0. The temperature was then decreased to 18 °C before expression of HaloTag was induced with 1 mM IPTG. The culture was grown for an additional 16 hours and was then centrifuged at 5000 x g for 20 minutes. Cell pellets were stored at -80 °C until purification.

HaloTagFusion Construct Purification

Cell pellets from 250 mL cultures were re-suspended in His6 Wash Buffer (50 mM HEPES pH 7.5, 10 mM imidazole) and PMSF (100 μg/mL) was added. Cells were lysed by sonication and centrifuged at 10,000 rpm for 20 minutes at 4 °C to clear the lysate. The cleared lysate was then added to 125 μL Promega HisLink™ Protein Purification resin and rotated at 4 °C for 30 minutes. The resin was washed with His6 Wash Buffer (3x), and the protein was then eluted with His6 Elution Buffer (Wash buffer with 600 mM imidazole). The collected fractions were then dialyzed into storage buffer (50 mM HEPES pH 7.5, 1 mM DTT), concentrated, and snap-frozen.

Mammalian lysate preparation

COS-7 cells were grown to confluency in 25 cm plates and harvested in pellets. Cell lysis buffer (50 mM Tris, 100 mM NaCl, 1 mM PMSF, PhosStop phosphatase inhibitor) was chilled on ice and then 1.5 ml of buffer was added to five combined pellets. The cells were lysed using a Dounce homogenizer. The lysate was cleared via centrifugation for 20 minutes at 16,000 rpm. Lysate concentration was determined using a Bradford assay.

Crosslinking time course

Purified kinase (25 nM), mammalian lysate (0.5 mg/ml) and HT-**1** (50 nM) were diluted in PBS in a 96-well, U-bottom plate. Samples were mixed and irradiated on ice at 365 nm by placing a Spectroline ENF-260C UV lamp directly on top of the plate. Samples were irradiated for various time points between 0 and 60 minutes and quenched with SDS loading buffer. Samples were separated by SDS-PAGE and visualized via Western blot

using an anti-SFK (36D10) antibody (Cell Signaling). The scanned blots were quantified with LI-COR Odyssey software to determine crosslinking efficiency.

Crosslinking to endogenous kinases in cells

COS-7 cells, grown in a 12-well plate, were transfected with a HaloTag fusion protein (pDEST26) using Fugene HD reagent (Promega). Cells grown to confluency were treated with 1 μM **1** in the absence or presence of 10 μM free dasatinib in a final volume of 1 ml of media (High glucose DMEM, 10% FBS with Strep/Pen). Treated cells were incubated for 1 hour at 37°C, washed with media (3x, 5 minutes at 37°C) and replaced with 1 ml PBS. Samples were irradiated at 365 nm at 37 °C for 8 minutes by placing a Spectroline ENF-260C UV lamp directly on top of the uncovered plate. After irradiation the PBS was aspirated and the cells were lysed with 1X SDS loading buffer containing PhosStop phosphatase inhibitor. Samples were separated on an SDS PAGE gel and visualized via Western blot using an anti-SFK (36D10) antibody (Cell Signaling).

Determining percent crosslinking efficiency for SFK variants

COS-7 cells, grown in a 12-well plate, were co-transfected with a HaloTag fusion protein (pDEST26) and the kinase of interest (pcDNA3.2-V5) using Fugene HD reagent (Promega). The cells were incubated at 37 °C for 24 hours. The transfected cells were treated with 1 μM of **1** in 1 ml of media (High glucose DMEM, 10% FBS with Strep/Pen) for 1 hour at 37°C. The cells were washed with media (3x, 5 minutes at 37 °C) and then 1 ml of PBS was added. The cells were irradiated at 365 nm at 37 °C for 8 minutes by placing a Spectroline ENF-260C UV lamp directly on top of the uncovered plate. After

irradiation the PBS was aspirated and the cells were lysed with 1X SDS loading buffer containing PhosStop phosphatase inhibitor. Samples were separated on an SDS PAGE gel and visualized via Western blot using an anti-V5 antibody (Sigma). The scanned blots were quantified with LI-COR Odyssey software to determine crosslinking efficiency using the following equation:

$$\text{Percent crosslinking efficiency} = \left(\frac{\text{Crosslinked kinase}}{\text{Non-crosslinked kinase + crosslinked kinase}} \right) \text{X } 100$$

Cellular IC_{50} Determination

COS-7 cells, grown in a 12-well plate, were co-transfected with a HaloTag fusion protein (pDEST26) and the kinase of interest (pcDNA3.2-V5) using Fugene HD reagent (Promega). The cells were incubated at 37 °C for 24 hours. The transfected cells were treated with 400 nM **1** and varying concentrations of competitor (10 μM – 0 μM, 3-fold dilutuions) for one hour at 37 °C. Cells were then irradiated at 365 nm at 37 °C for 8 minutes by placing a Spectroline ENF-260C UV lamp directly on top of the uncovered plate. After irradiation, the media was aspirated and the cells were lysed with 1X SDS loading buffer containing PhosStop phosphatase inhibitor. Samples were separated on an SDS-PAGE gel and visualized via Western blot using an anti-V5 antibody (Sigma). The scanned blots were quantified with LI-COR Odyssey software and converted to percent inhibition. Data was analyzed using Prism Graphpad software and IC_{50} values were determined using non-linear regression analysis.

Crystallography

A 20 mM stock solution of inhibitor **9** (in 100% DMSO) was added to SRC (final concentration = 2 mM). This mixture was incubated on ice for approximately one hour and spun down to remove insoluble compound prior to setting up the crystallization experiment. Crystals were grown at room temperature by vapor diffusion from a sitting drop containing 0.8 μL SRC-**9** solution (5.4 mg/ml protein, 100 mM NaCl, 5% glycerol, 1 mM DTT, 25 mM Tris pH 8.0, 2 mM inhibitor **9**, 10% DMSO) plus 0.7 μL crystallization buffer (6% PEG 20K, 100 mM MES pH 6.5). Diffraction images were measured at SSRL Beamline 12.2 at an X-ray wavelength of 0.9795 Å and processed using Mosflm and the CCP4 program suite. The initial structural model was taken from PDB entry 2OIQ and refined using alternating rounds of manual fitting in Coot and automated refinement in Refmac. Model geometry was validated using Molprobity, which reported 97.5% of the residues as lying in favorable regions of φ/ψ space, with no outliers. Crystallographic statistics are shown in **Supplementary Table 2**. The final model has been deposited with the PDB as entry **4DGG**.

Fluorescence Polarization Assay

100 nM of FAM-AAVSLARRPLPPLP-NH_2 was incubated with varying concentrations of SRC^{Y527F} or HCK^{Y527} in the presence of a saturating concentration of dasatinib or inhibitor **10**. 30 μM dasatinib or 60 μM **10** was included in every well. All components were incubated in buffer containing 10 mM phosphate, 25 mM Tris, pH 7.8, 0.5 mM EDTA, 175 mM NaCl, 0.1 mM NaN_3, and 0.025% pluronic acid (final volume = 60 μL per well) at room temperature for 1 hour prior to reading. Data were analyzed using

Prism Graphpad software and K_d values were determined using non-linear regression analysis. Values shown are the average of three assays ± SEM.

Supplemental References:

1. Cheng, Y. & Prusoff, W. H. Relationship between the inhibition constant (K_1) and the concentration of inhibitor which causes 50% inhibition (I_{50}) of an enzymatic reaction. *Biochem. Pharmacol.* **22**, 3099−3108 (1973).

2. Holt, D. A. *et al.* Benzophenone- and Indolecarboxylic Acids: Potent Type-2 Specific Inhibitors of Human Steroid 5.alpha.-Reductase. *J. Med. Chem.* **38**, 13-15 (1995).

3. Fischer, J. J. *et al.* Dasatinib, imatinib and staurosporine capture compounds — Complementary tools for the profiling of kinases by Capture Compound Mass Spectrometry (CCMS). *J. Proteomics* **75**, 160-168 (2011).

4. Krishnamurty, R. & Maly, D.J. Protein kinase affinity reagents based on a 5-aminoindazole scaffold. *Bioorg. Med. Chem. Lett.* **21**, 550-554 (2010).

5. Johnson, S. M. *et al.* Development of Toxoplasma gondii calcium-dependent protein kinase 1 (TgCDPK1) inhibitors with potent anti-toxoplasma activity. *J. Med. Chem.* **55**, 2416-2426 (2012).